Penerbit Akademia Baru

Journal of Advanced Research in Fluid Mechanics and Thermal Sciences

Journal homepage: www.akademiabaru.com/arfmts.html
ISSN: 2289-7879

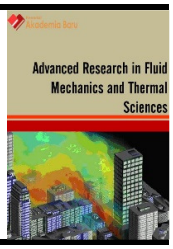

Numerical Study of Aerodynamic Performance of Hatchback Vehicle Fitted with a Strip Spoiler: Effect of Yaw Angle

Open Access

See-Yuan Cheng[1,2,*], Shuhaimi Mansor[3], Mohd Azman Abdullah[1,2], Mohamad Shukri Zakaria[1,2]

[1] Centre for Advanced Research on Energy, Universiti Teknikal Malaysia Melaka, Hang Tuah Jaya, 76100 Durian Tunggal, Melaka, Malaysia
[2] Faculty of Mechanical Engineering, Universiti Teknikal Malaysia Melaka, Hang Tuah Jaya, 76100 Durian Tunggal, Melaka, Malaysia
[3] Faculty of Mechanical Engineering, Universiti Teknologi Malaysia, 81310 UTM Skudai, Johor, Malaysia

ARTICLE INFO

Article history:
Received 30 April 2018
Received in revised form 30 June 2018
Accepted 10 July 2018
Available online 23 July 2018

Keywords:
Spoiler, hatchback, yaw angle, aerodynamics, CFD

ABSTRACT

This study investigated the effect of yaw angle on the aerodynamic performance of hatchback vehicle model fitted with a strip spoiler. Conventionally, the performance of rear-roof spoilers had mainly been optimized for straight-ahead driving condition. However, during cornering, the effect of spoiler is most needed to ensure that the vehicle can drive through the curve without slip. Hence, this study aims to investigate the effects of yaw angle change corresponding to cornering on the flow characteristics of strip spoiler, and the subsequent influence on the aerodynamic performance of hatchback vehicles. A RANS-based computational fluid dynamics (CFD) method was used. A simplified hatchback model was adopted. The numerically obtained results was compared to the experimental data for validation of the CFD method. It was found that both the lift and drag coefficient of the spoiler were to increase with increasing yaw angle. Similarly, the overall Cd and C_l of the model were also increased with increasing yaw angle. The main body parts that contributed to the increase in C_d are the base and slant, whereas the front tended to attenuate the C_d. Meanwhile, the rise in C_l was mainly caused by the roof, and resisted by the underbody.

1. Introduction

A spoiler is an external structured added to the trailing edge of the roof of a vehicle to increase the downward force, and hence, improves its traction. To date, the performance of spoilers had mainly been optimized for straight-ahead driving condition. However, during cornering, good traction is critical to ensure that sufficient centripetal force is generated for the vehicle to drive through the curve without slip. Hence, this study aims to investigate the effects of yaw angle change corresponding to cornering on the flow characteristics of rear-roof spoiler, and the subsequent influence on the aerodynamic performance of hatchback vehicles.

Generally, there are two rear spoiler types: strips and free-standing wing. The effectiveness of wing-type spoiler has been reported in numerous studies [1-11]. For instance, Kim *et al*., [4] revealed

* *Corresponding author.*
E-mail address: cheng@utem.edu.my (See-Yuan Cheng)

that the use of a rear spoiler on a mini-van has successfully reduced the lift by more than 100% when the mini-van is moving at the speed of 108 km/h. As for car, Tsai *et al.*, [5] has employed various wing spoilers to study their effects on a simple bluff body inspired by the HONDA S2000. They reported reductions in the lift force for all the spoiler types investigated. On a similar note, Daryakenari *et al.*, [3] has reported up to 75% drop in the lift coefficient when the incident angle of the spoiler mounted on a passenger car model was set correctly. In addition, Kodali and Bezavada [12] has produced lower lift coefficient with the wing spoiler at up to 80%. In the case of strip spoiler, a study about its effect on the crosswind stability and drag force for Ahmed body with a backlight angle of 35° has been carried out by Menon *et al.*, [13]. However, the lift force was not being considered in their study.

Notably, the scopes of these studies [3-5, 12-13] are limited to zero degree yaw angle, i.e. the oncoming flow approached the spoiler in the longitudinal direction of the vehicle, which simulates a straight-ahead driving condition. However, in practice, the effect of spoiler is most needed during cornering (i.e. none zero yaw angle) to ensure ride safety by providing better downforce. The spoilers being designed for straight-ahead driving may become less effective during cornering, due to the fact that the air is no longer passing exactly fore-aft (i.e. none zero yaw angle). In fact, the yaw angle could increase to about 10° [14]. Hence, it is important to understand the flow and aerodynamic characteristics of spoiler at a range of yaw angle corresponding to flow conditions during cornering.

Although the effect of spoiler at the yaw angle of 30° has been investigated by Menon *et al.*, [13], however, its aim was on side wind stability. The results obtained from only one yaw angle are insufficient to describe the aerodynamic characteristics of spoiler during cornering. In addition, most of the studies had investigated the effect of wing spoiler. The literature on the effects of strip type spoiler is scarce. To fill the gap, hence, the main objective of the present paper is to investigate the effect of yaw angle on the aerodynamic performance of simplified hatchback model mounted with a strip-type rear-roof spoiler.

2. Methodology

2.1 Hatchback Model and Spoiler Configurations

The Ahmed body [15] which represents simplified road vehicle geometry in the form of a bluff body was adopted. The slant angle was at 35°, which is typical for most hatchback cars (see Figure 1). The use of simplified model is to prevent interference effect among body parts which would otherwise been found on real vehicles. This approach has been implemented successfully in many studies concerning automotive aerodynamics (e.g. [15-20]). As shown in the figure, a roof spoiler was attached at the roof-slant junction. The incident angle of the spoiler was at 5°. The yaw angle convention is also depicted in the figure. The angle ranges from 0° to 12°, at an increment of 4°.

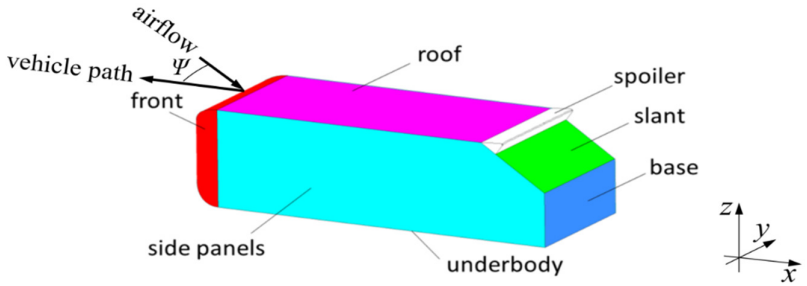

Fig. 1. Ahmed model fitted with a rear-roof spoiler and the convention of yaw angle

The roof spoiler was 70% shorter than the slant, which means it was 66.6 mm long. We filleted the end of the spoiler which has a sharp angle to avoid generating problematic cells in the meshing process. The fillet setting was at 5 mm radius. In addition, the back of the spoiler which protruded from the slant surface has been kept perpendicular to the slant.

2.2 Computational Method

2.2.1 Numerical settings

The present study solved the Reynolds-averaged Navier-Stokes (RANS) equations by a commercial CFD solver, namely ANSYS Fluent 16. It utilizes a finite-volume method. The flow is assumed incompressible as the Ma is well below 0.3. The time-averaged mass and momentum equations solved are as following:

$$\frac{\partial \mathrm{u_i}}{\partial \mathrm{x_i}} = 0 \tag{1}$$

$$\rho u_j \frac{\partial u_i}{\partial x_i} = \frac{\partial}{\partial x_i}\left[-p\delta_{ij} + 2\mu S_{ij} - \rho u'_i u'_j\right] \tag{2}$$

where,

ρ	= density of fluid
u	= time-averaged velocity
p	= time-averaged static pressure
μ	= viscosity of fluid
S_{ij}	= mean rate of strain tensor
$\rho u'_i u'_j$	= Reynolds stresses

The Reynolds stresses which represent the turbulent effects were modelled by the k-epsilon realizable model to close equation (2). In the case when the first grid point is within the range of logarithmic layer, the wall function is used to model the boundary layer profile. Subsequently, the surface friction is estimated. The steady state, pressure-based solver was used. Moreover, the upwind scheme of second-order accuracy was used for discretization.

The domain has a rectangular cross section (1742.9 mm high and 4407.6 mm wide) and is 13.8*l* long (*l* is the length of the vehicle model, which is equaled to 1.044 m). The blockage ratio of the flow was below 1.5%. Thus, the value is within the typical acceptable range of 5% in automotive aerodynamic testing [13].

The inlet boundary was located at 1.4*l* upstream of the model while the outlet boundary was at 11.4*l* downstream. A uniform velocity of 40 m/s was assigned at the inlet, while the outlet was set at zero gauge pressure. The height-based Re of the flow was 768,000. Symmetry boundary condition was used for the ceiling and side walls of the domain, while no-slip condition was applied to the domain floor and the model surfaces.

2.2.1 Meshing

Figure 2 shows the cell types and mesh density of the domain. As depicted, finer cells were used on the model surfaces and the cells were progressively becoming coarser as they extended outward towards the domain boundaries. In addition, prismatic cells were used near the model surfaces and the floor. The first node distance from the model surface was fixed at 0.5 mm. This setting yields small y+ values on the model surfaces, which range from about 1.2 to 80. Grid independence test has

been performed to check the effect of mesh size. It was found that the grid at about 1403904 elements is adequate.

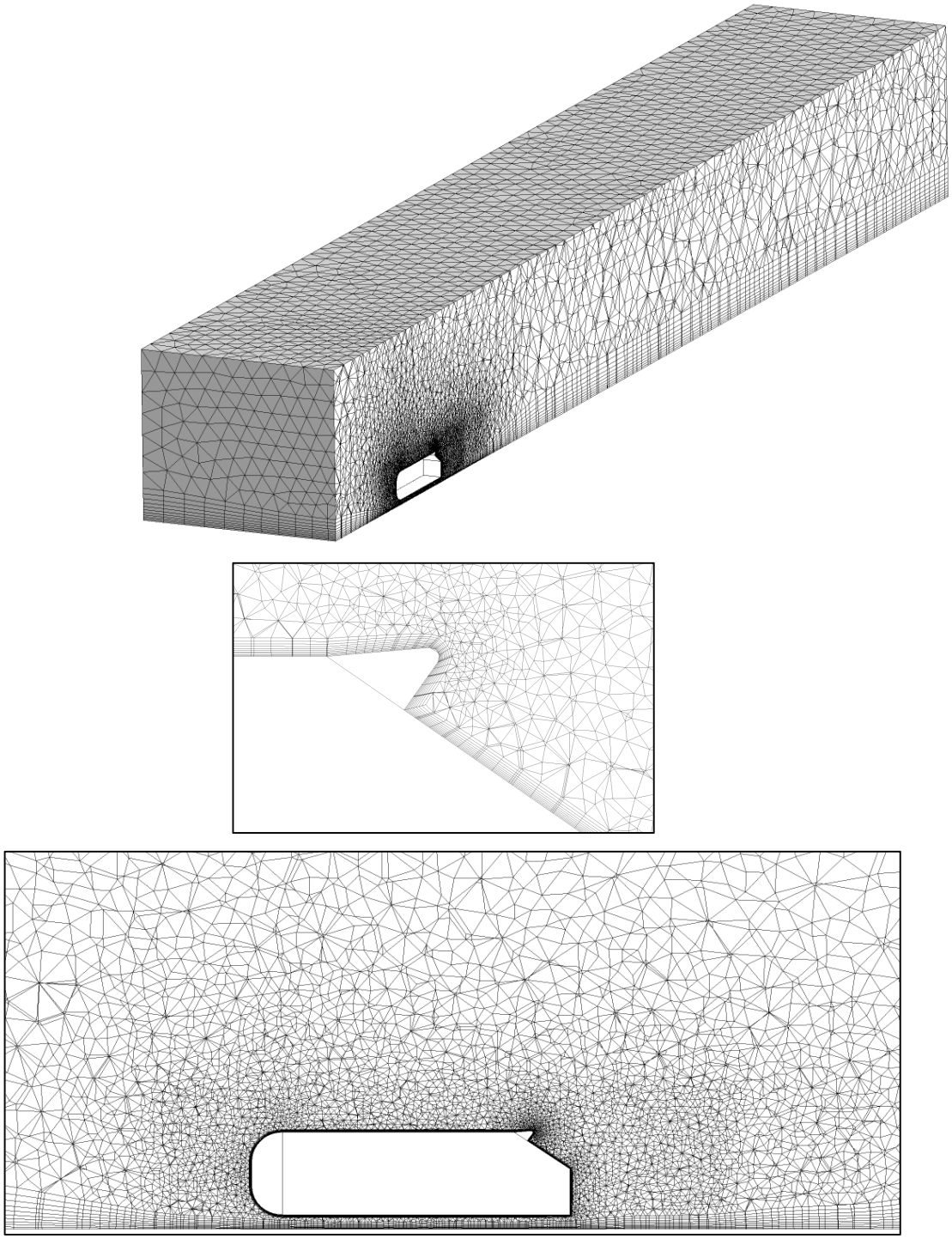

Fig. 2. Numerical cells of the simulation domain (top), close-up of prismatic cells around the rear-roof spoiler (middle), and mesh density distribution around the Ahmed body (bottom)

2.2.2 Validation

We validated the CFD model against the wind tunnel data available in the literature. The Re used in the validation was 768,000. This value was selected based on the setting used by Lienhart et al. [16]. We observed that the CFD model has reproduced the flow features well, particularly at the rear section of the Ahmed body. These features include the separation at the trailing edge of the roof, and the recirculating bubble in the wake of the Ahmed body. Similar flow pattern has also been reported in the literature (e.g. [15-17]).

Quantitatively, the percentage difference in C_d was about 6.5% as compared to the result obtained by Lienhart *et al.*, [16]. Because no attempt was made to reproduce exactly the experimental conditions of Lienhart *et al.*, [16], this level of agreement is quite reasonable.

3. Results and Discussion

3.1 Effect of Yaw Angle on C_d and C_l

Figure 3(a) shows that both the C_d and C_l of the model had increased with increasing yaw angle. Note that the present study has adopted the body-axis system, i.e., C_d is defined as the aerodynamic force component parallel to the longitudinal axis of the model. Also shown in the figure are the influence of yaw angle on the spoiler contribution to C_d and C_l (Figure 3(b)). As depicted, its contribution to C_d and C_l had increased with increasing yaw angle. This tendency means that its effectiveness in improving the vehicle's fuel efficiency and running stability were to deteriorate in none-zero-yaw conditions, such as when the vehicle is subjected to crosswinds or when it no longer travels in a straight path.

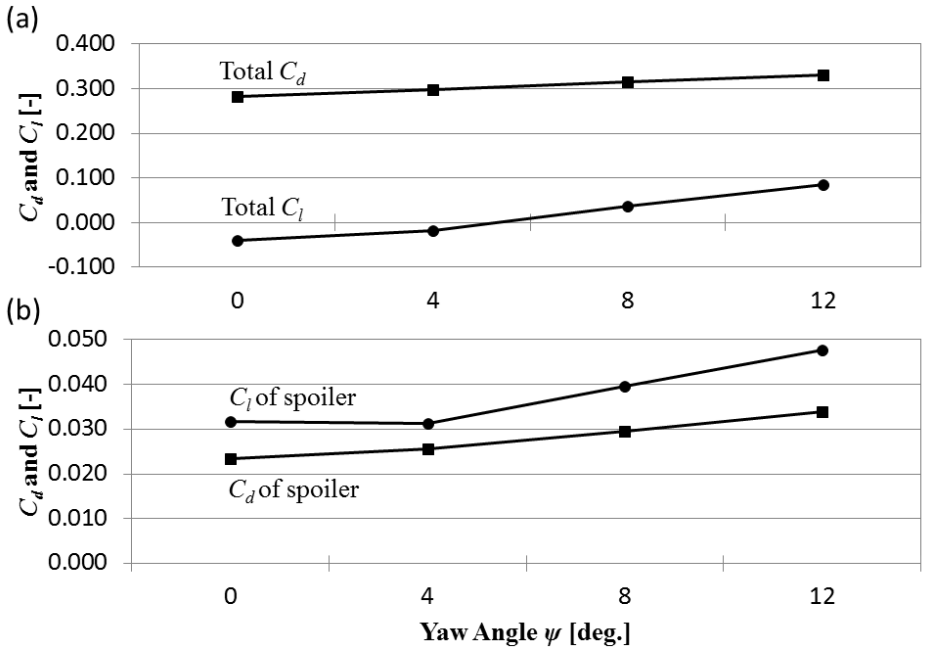

Fig. 3. Effect of yaw angle on C_d and C_l

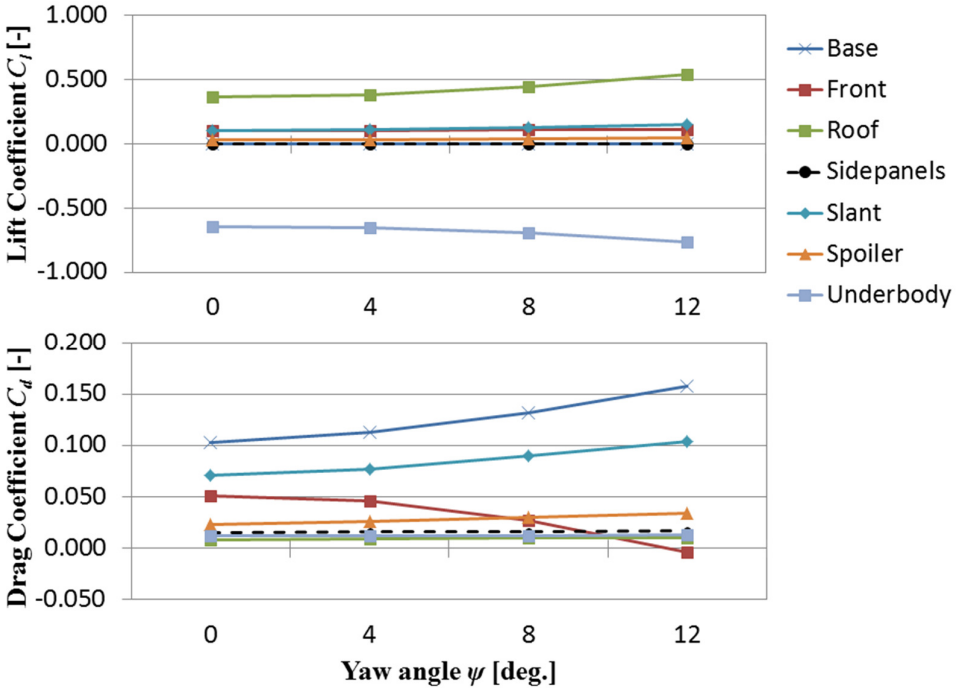

Fig. 4. Effect of yaw angle on body part contributions to C_d and C_l

Figure 4(a) reveals that the C_l contribution from the base and underbody were most significant when the model is subjected to yaw angle. These two body parts had the opposite influences with the former exerting a negative one. Meanwhile, the base, slant, and front were most significant in affecting the Cd with the latter showing a desirable influence. The physical mechanism on how the C_d and C_l of these body parts are being influenced by yaw angle change is given in the following subsections.

3.2 Effect of Yaw Angle on Flow Structures

When the model was subjected to yaw angles, four longitudinal vortices (marked A, B, C, and D in Figure 5) were generated which emanated at the four front corners of the model. The generation of these vortices is reasonable considering that the front corner edges are of angular shape. When viewed from the back of the model, the upper and lower vortex pairs had the counter clockwise and clockwise rotations, respectively (see Figure 5). These vortices propagated downstream alongside the model with decreasing intensity but their vortex rings were widened (see Figure 6).
As shown in Figure 5, the paths of the windward vortices A and B are respectively, located on the top and bottom of the model near the windward side. However, the paths of the leeward vortices C and D are located away from the model surfaces. Consequently, the windward vortices could influence the surface pressure of the model especially at higher yaw angle due to increasing vortex strength. Figure 6 shows that the intensity and size of vortices A, B, C, and D (depicted by the Q criterion contour) were to increase with increasing yaw angle.

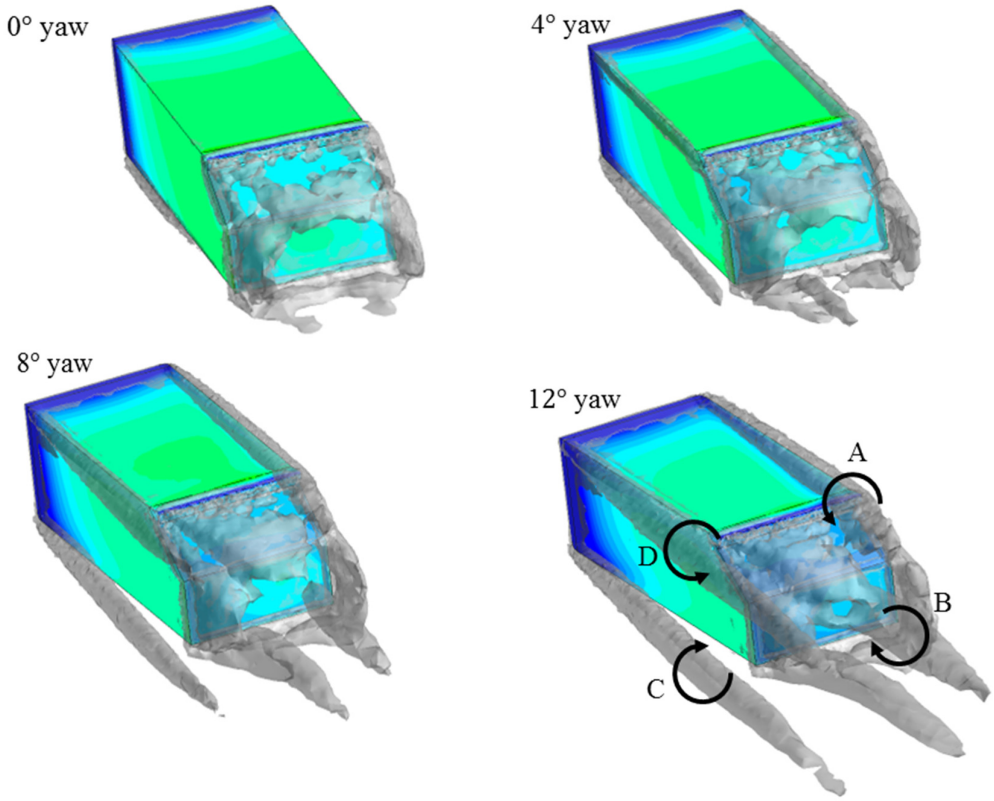

Fig. 5. Effect of yaw angle on body part contributions to C_d and C_l

3.3 Physical Mechanism

Figure 7 compares the surface pressure distribution on the top and bottom of the model at increasing yaw angles. As may be seen, the windward vortices had induced the low surface pressure regions along the top and bottom surfaces of the model (region in the red box). Since the decrease in the surface pressure of the roof could cause the C_l to increase, therefore the contribution of C_l from the roof had shown an increase tendency. On the other hand, the decrease in the surface pressure of the underbody would cause the C_l to decrease; hence the underbody had a favorable contribution – improving downforce.

The reason for reduction in C_d for the front part contribution is because of the widening of the low surface pressure region near the leeward side of the front part (i.e. left vertical edge) with increasing yaw angle (see Figure 8). Figure 9 shows that the widened low surface pressure region is associated with the flow acceleration near the leeward side corner at higher yaw angle.

Meanwhile, the reason for the drop in the surface pressure of the slant and base at higher yaw angle which has contributed to the increase in C_d, is associated with the formation of significant crossflow behind the model (see Figure 10). These crossflow structures are the result of vortex shedding at higher yaw angle.

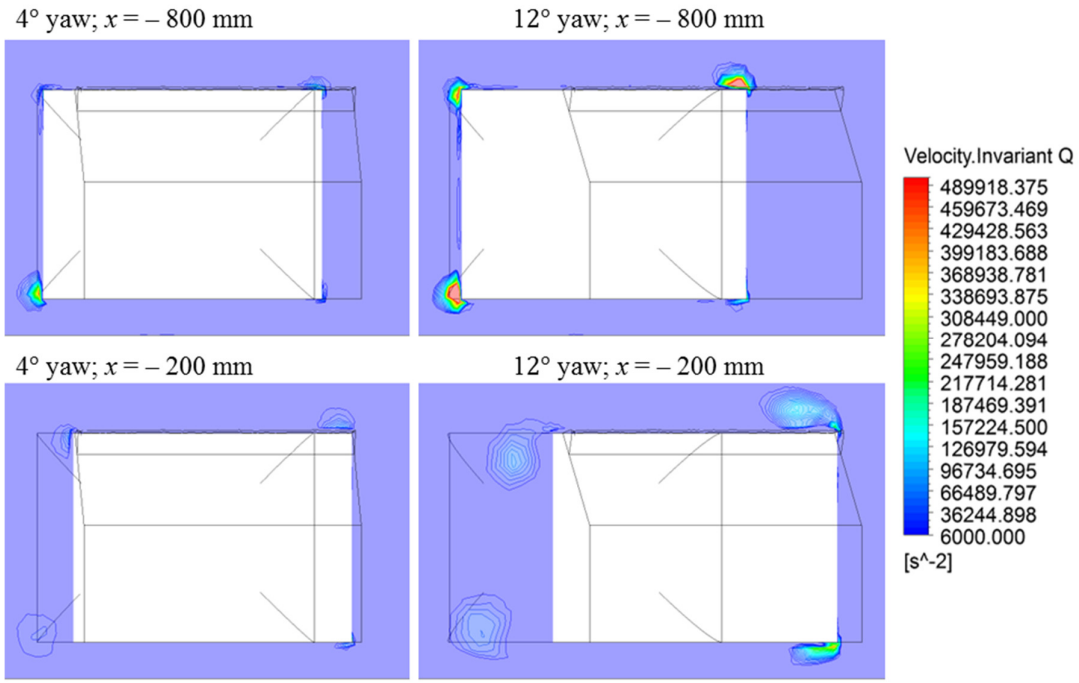

Fig. 6. Yaw angle effect on longitudinal vortices; comparison between the Q criterion obtained from 4° and 12° yaw angles

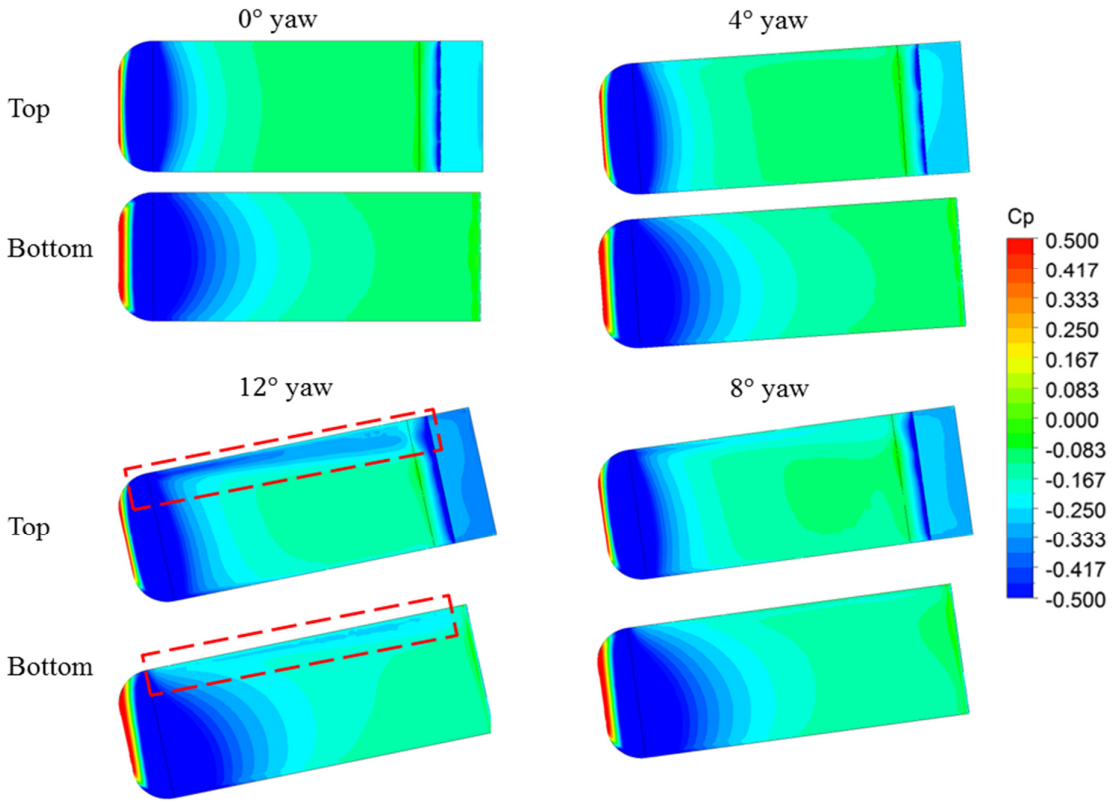

Fig. 7. Yaw angle effect on surface pressure distribution

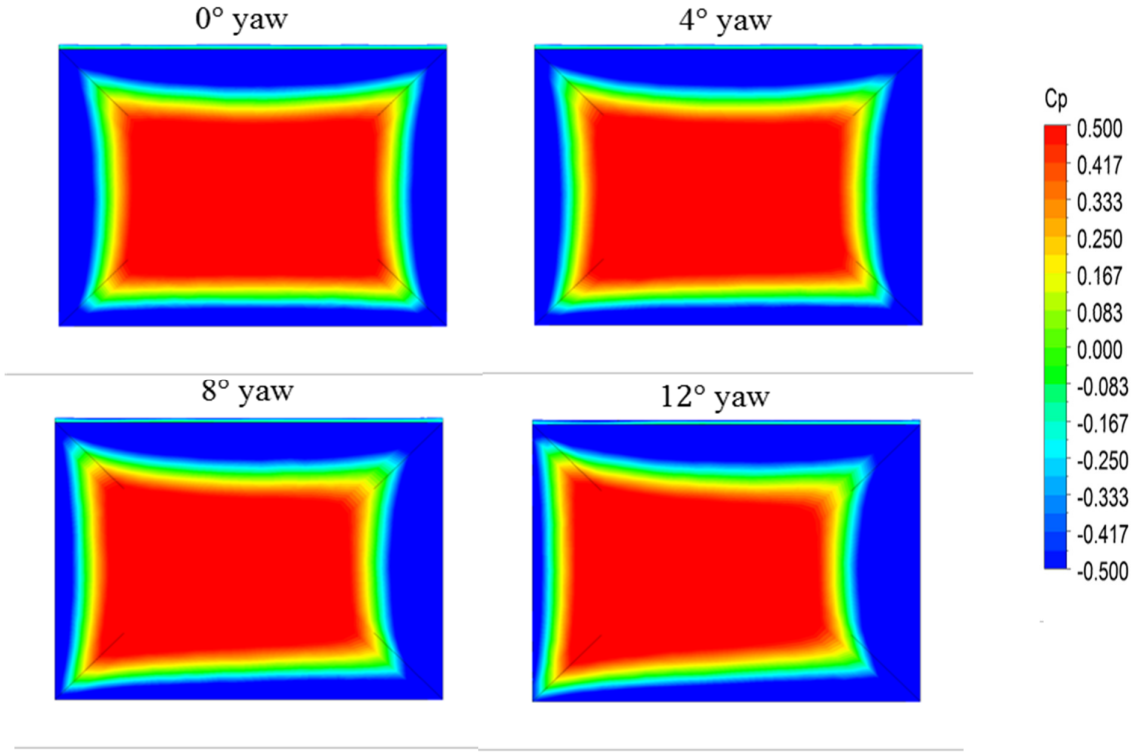

Fig. 8. Yaw angle effect on the surface pressure distribution of the front part

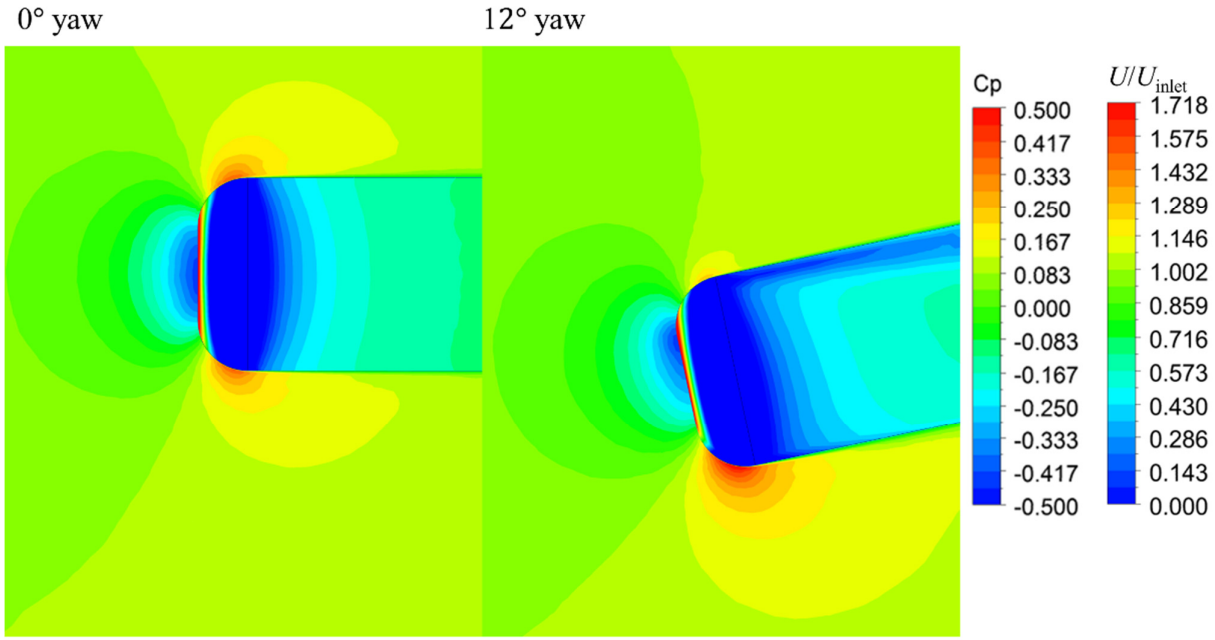

Fig. 9. Yaw angle effect on the velocity distribution near the front part; visualization plane at the mid height of the model.

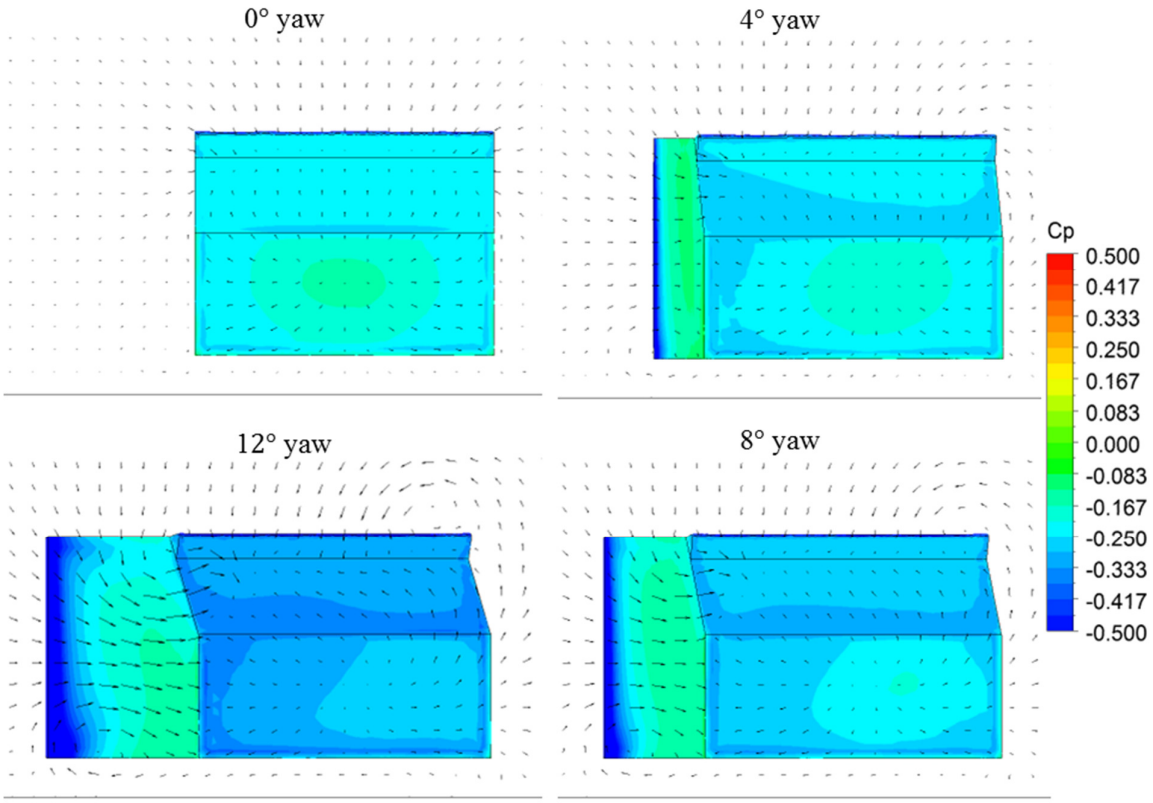

Fig. 10. Yaw angle effect on the surface pressure distribution of the rear section

4. Conclusion

This paper investigated the effect of yaw angle on the aerodynamic performance of hatchback vehicle model fitted with a rear-roof spoiler by a RANS-based CFD method. The results show that both the lift and drag coefficient of the spoiler were to increase with increasing yaw angle – deterioration tendency. In addition, the overall C_d and C_l of the model were also increased with increasing yaw angle. The main body parts that contributed to the increase in C_d are the base and slant, whereas the front tended to attenuate the C_d. Meanwhile, the rise in C_l was mainly caused by the roof, and resisted by the underbody.

Acknowledgement

The authors would like to thank Universiti Teknikal Malaysia Melaka (UTeM) and Ministry of Higher Education for supporting this research under FRGS FRGS/1/2015/TK03/FKM/02/F00273.

References

[1] Cheng, S. Y., and S. Mansor. "Rear-roof spoiler effect on the aerodynamic drag performance of a simplified hatchback model." In *Journal of Physics: Conference Series*, vol. 822, no. 1, p. 012008. IOP Publishing, 2017.

[2] Cheng, See-Yuan, and Shuhaimi Mansor. "Influence of rear-roof spoiler on the aerodynamic performance of hatchback vehicle." In *MATEC Web of Conferences*, vol. 90, p. 01027. EDP Sciences, 2017.

[3] Daryakenari, Behrang, Shahrir Abdullah, Rozli Zulkifli, E. Sundararajan, and AB Mohd Sood. "Numerical study of flow over ahmed body and a road vehicle and the change in aerodynamic characteristics caused by rear spoiler." *International Journal of Fluid Mechanics Research* 40, no. 4 (2013).

[4] Kim, Inchul, Hualei Chen, and Roger C. Shulze. *A rear spoiler of a new type that reduces the aerodynamic forces on a mini-van*. No. 2006-01-1631. SAE Technical Paper, 2006.
[5] Tsai, Chien-Hsiung, Lung-Ming Fu, Chang-Hsien Tai, Yen-Loung Huang, and Jik-Chang Leong. "Computational aero-acoustic analysis of a passenger car with a rear spoiler." *Applied Mathematical Modelling* 33, no. 9 (2009): 3661-3673.
[6] Kieffer, W., S. Moujaes, and N. Armbya. "CFD study of section characteristics of Formula Mazda race car wings." *Mathematical and Computer Modelling* 43, no. 11-12 (2006): 1275-1287.
[7] Mitra, D. E. B. O. J. Y. O. T. I. "Effect of relative wind on notch back car with add-on parts." *International Journal of Engineering Science and Technology* 2, no. 4 (2010): 472-476.
[8] Hu, X. X., and T. T. Wong. "A numerical study on rear-spoiler of passenger vehicle." *World Academy of Science, Engineering and Technology* (2011).
[9] Hu, X. X., and T. T. Wong. "A numerical study on rear-spoiler of passenger vehicle." *World Academy of Science, Engineering and Technology* (2011).
[10] Tousi, S. M. R., and P. Bayat. "Evaluating the Importance of Rear Spoiler on Energy Efficiency of Electric Vehicles." *International Journal of Automotive Engineering* 5, no. 4 (2015): 2034-2053.
[11] Chin, K. Y., Cheng, S. Y., and Mansor, S. "Yaw Angle Effect on the Aerodynamic Performance of Hatchback Vehicle Fitted with Combo-Type Spoiler." *Journal of Advanced Research in Fluid Mechanics and Thermal Sciences* 44 (2018): 1-11.
[12] Kodali, Shyam P., and S. R. I. N. I. V. A. S. Bezavada. "Numerical simulation of air flow over a passenger car and the Influence of rear spoiler using CFD." *International Journal of Advanced Transport Phenomena* 1, no. 1 (2012): 6-13.
[13] Menon, D. P., Kamat G, S., Mukkamala, Y. S., and Kulkarni, P. S. 2014. To improve the aerodynamic performance of a model hatchback car with the addition of a rear roof spoiler. 16th Annual CFD Symposium, August 11-12, 2014, Bangolore.
[14] Hucho, W-H. ed. 1998. Aerodynamics of road vehicles. Fourth edition. Warrendale, PA: SAE International.
[15] Ahmed, Syed R., G. Ramm, and G. Faltin. "Some salient features of the time-averaged ground vehicle wake." SAE Transactions 93 (1984): 473-503.
[16] Lienhart H., Stoots C., and Becker S. 2000. Flow and turbulence structures on the wake of a simplified car model (Ahmed model), DGLR Fach. Symp. der AG ATAB, Stuttgart University.
[17] Vino, G., S. Watkins, P. Mousley, J. Watmuff, and S. Prasad. "Flow structures in the near-wake of the Ahmed model." *Journal of fluids and structures* 20, no. 5 (2005): 673-695.
[18] Cheng, S. Y., Makoto Tsubokura, Takuji Nakashima, Takahide Nouzawa, and Yoshihiro Okada. "A numerical analysis of transient flow past road vehicles subjected to pitching oscillation." *Journal of Wind Engineering and Industrial Aerodynamics* 99, no. 5 (2011): 511-522.
[19] Cheng, S. Y., M. Tsubokura, T. Nakashima, Y. Okada, and T. Nouzawa. "Numerical quantification of aerodynamic damping on pitching of vehicle-inspired bluff body." *Journal of Fluids and Structures* 30 (2012): 188-204.
[20] Shaharuddin, N. H., Mat Ali, M. S., Mansor, S., Muhamad, S., Shaikh Salim, S. A. and Usman, M. "Flow simulations of generic vehicle model SAE type 4 and DrivAer Fastback using OpenFOAM." *Journal of Advanced Research in Fluid Mechanics and Thermal Sciences* 37, (2017): 18-31.